UV-Curable Hybrid Coatings Based on Vinylfunctionlized Siloxane Oligomer and Acrylated Polyester

Jianyun He,[1] Liang Zhou,[1] Mark D. Soucek,[1] Kathleen M. Wollyung,[2] Chrys Wesdemiotis[2]

[1]*Department of Polymer Engineering, University of Akron, Akron, Ohio 44325*
[2]*Department of Chemistry, University of Akron, Akron, Ohio 44325*

Received 7 March 2006; accepted 7 May 2006
DOI 10.1002/app.25709
Published online 8 May 2007 in Wiley InterScience (www.interscience.wiley.com).

ABSTRACT: Organic–inorganic hybrid coatings were formulated using multifunctional vinyltrimethoxysilane (VTMS) oligomers and acrylated polyester (AP). A radical photoinitiator was added to the VTMS/AP formulation and the films were crosslinked via UV-radiation. The viscoelastic, thermomechanical, and surface properties of the VTMS/AP films were evaluated as a function of VTMS content, using dynamic mechanical thermal analysis (DMTA), thermal gravimetric analysis (TGA), contact angle, fracture toughness, and tensile properties. In addition, coating properties such as adhesion, scratch resistance, pencil hardness, and impact resistance were also investigated. The tensile and scratch data show that VTMS oligomer dramatically increased hardness and scratch resistance. The VTMS oligomer also increased the contact angle, led to a decrease in surface tension, and improved surface appearance. The VTMS oligomer also increases storage modulus, glass transition temperature, and crosslink density. The morphology of films and the particle size were observed using atomic force microscopy (AFM). The data indicated that the average silica particle size was ~90 nm and the particles were well-dispersed in the organic phase. It was postulated that the VTMS oligomer functioned effectively as a hyperbranched crosslinker, surface modifier, and reactive diluent. J Appl Polym Sci 105: 2376–2386, 2007

Key words: vinyltrimethoxysilane; multifunctional oligomer; acrylated polyester; UV-curing; organic–inorganic hybrid film; hyperbranched crosslinker; surface modifier; reactive diluent

INTRODUCTION

In recent years, organic–inorganic hybrid materials have received considerable attention as new functional materials.[1–8] Generally, the hybrid material is formed through the hydrolysis and condensation of organically modified silicates. These materials are of great interest since they impart both organic and inorganic characteristics. The organic component usually accounts for flexibility of the composites, whereas the inorganic component is responsible for hardness and mechanical impact resistance.[9] Organic–inorganic hybrid coating provides some properties to the substrate, such as wear, corrosion, erosion, optical, magnetic, electric–electronic, biological, and thermal attack properties. These properties of the coatings are very important in surface engineering applications. It also the aim of decorative attractiveness for the surface.[10]

The sol–gel process from precursors is attractive in a number of academic studies and commercial application, because it provides low processing temperature, high material purity, and relative low cost.[11] The sol–gel process can be either acid or base catalyzed. In the sol–gel process, metal alkoxides as a sol–gel precursor produces a condensed film barrier layer on the metal substrate through the hydrolysis and condensation reaction. Silicon alkoxide is the most used sol–gel precursor that is used both as corrosion inhibitor and as adhesion promoter. Usually, both hydrolysis and condensation of silicon alkoxide in the sol–gel method can occur by acid- or base-catalyzed bimolecular nucleophilic substitution reactions. At low pH level (acid catalyst) where hydrolysis is fast, the silica tends to form a linear link that occasionally crosslinks. These molecular chains entangle and form additional branches resulting in gellation. At high pH level (base catalyst), which is the conventional base–catalyzed process where condensation is fast, highly branched clusters are formed and the gelation occurs by linking of clusters. Nanoparticles based on the silicon–titanium system can be prepared by the sol–gel method which includes hydrolysis and condensation of alkoxysilanes in a liquid solution as described below:

Hydrolysis:

$$\equiv \mathrm{Si}(\mathrm{OC_2H_5}) + \mathrm{H_2O} \rightarrow \equiv \mathrm{Si\text{-}OH} + \mathrm{C_2H_2OH}$$

Correspondence to: M. D. Soucek (msoucek@uakron.edu).

Journal of Applied Polymer Science, Vol. 105, 2376–2386 (2007)

Water condensation:

$$\equiv \text{Si-OH} + \text{HO-Si} \equiv \rightarrow \equiv \text{Si-O-Si} \equiv + \text{H}_2\text{O}$$

Alcohol condensation:

$$\equiv \text{Si}(\text{OC}_2\text{H}_5) + \text{HO-Si} \equiv \rightarrow \equiv \text{Si-O-Si} \equiv + \text{C}_2\text{H}_5\text{OH}$$

UV-light curable system is assuming increasing importance in the field of coatings in various industrial applications because of their peculiar characteristics and advantages with respect to the thermal and solvent based coatings. Over all, the most important features of this new technology can be summarized as follows: (a) solvent free process; (b) the curing reaction is very fast and can be controlled; (c) instant start and shut down; (d) the curing reaction takes place at room temperature; (e) lower energy consumption than thermal curing; (f) high production line with minimum working space, i.e., highly efficient; and (g) environmental friendly process technology. UV-curable resins usually consist of oligomers and multifunctional comonomers, which photopolymerize to form highly crosslinked polymeric networks and photoinitiators, which yield reactive initiating species when exposed to UV light. As a class of UV-curable oligomers, acrylic polyester has attracted increasing attention both from a fundamental viewpoint and for the great variety of expected applications.[12–20] Tetraethoxysilane (TEOS) precursor is one of the most commonly used precursors for the UV-light curable system.[21–25] It was found that the additional TEOS could enhance adhesion, corrosion, modulus, tensile strength, and hardness when the continuous organic phase was epoxy, polyester, polyurethane, and or epoxynorbornane linseed oil.[26–31]

However, the need for rapid cure materials with improved properties stimulated researchers to develop novel functional siloxane monomers or oligomers suitable for curable organic and inorganic hybrid materials. Our previous research reported that vinyltrimethoxysilane (VTMS) can be used to prepare vinyl functional silica-colloids by the sol–gel method.[11] Gunji et al. prepared polyvinylpolysilsesquioxane organic–inorganic hybrid gel films containing polyethylene and siloxane backbone linkages through the radical polymerization of vinyltrimethoxysilane followed by the acid-catalyzed hydrolytic polycondensation of trimethoxysilyl groups.[6] Polyvinylpolysilsesquioxane gel films were transparent and homogeneous. Hu et al. measured hardness and elastic modulus profiles of thin organic/inorganic hybrid coatings on glass surfaces with a continuous stiffness measurement technique. Hybrids were synthesized by the hydrolytic condensation of vinyltrimethoxysilane, with 5–30 wt % TEOS, in the presence of formic acid.[32]

The factors that determine the coating properties are the constitution of material composition of material composition parameters such as coating process and thickness, etc. By varying these factors, the properties of resistance to corrosion, flame, bond strength, and wear strength of polymeric based coating can be changed and the service life can be increased. A UV-curable acrylated polyester shows good properties such as high hardness, toughness, solvent resistant, and an excellent ratio value of properties to cost.[33] Therefore, it has been widely used as a binder for UV-curable films. In this study, organic–inorganic materials were prepared using vinyl functional silica-colloids VTMS and acrylated polyester. The backbone of acrylated polyester is composed of mostly linear segments with random cycloaliphatic segments, which provide a good balance of hardness, flexibility, and application viscosity. On the basis of our literature review, we believe that research presented here is compositionally and structurally unique; organic–inorganic hybrid materials based on acrylated polyester have not been previously reported in the literature.

In this study, multifunctionalized VTMS oligomers were prepared *ex situ* by the sol–gel method and UV-cured with an acrylated polyester. The effects of the concentration of VTMS oligomer on the coating properties such as adhesion, scratch resistance, pencil hardness, and impact resistance were investigated. In addition, the mechanical, viscoelastic, thermomechanical, and surface properties of the hybrid films were also evaluated using tensile strength, fracture toughness, dynamic mechanical thermal analysis (DMTA), thermal gravimetric analysis (TGA), contact angle, and pull-off adhesion.

EXPERIMENTAL

Materials

Vinyltrimethoxysilane (VTMS), hydrochloric acid (37 wt %), ethanol, 1,4-cyclohexane dimethanol (1,4-CHDM), neopentyl glycol (NPG), 1,6-hexanediol (1,6-HD), maleic anhydride (MA), adipic acid (ADA), acrylic acid (AA), dibutyltin oxide (98 wt %), *p*-toluenesulfonic acid monohydrate, and hydroquinone were purchased from Aldrich. The photoinitiator, Darocur 4265, were obtained from Ciba Specialty Chemical. All chemicals were used as received.

Preparation of VTMS oligomer

Vinyltrimethoxysilane (VTMS) was hydrolyzed with water by a sol–gel method. The VTMS (29.6 g, 0.2 mol) was dissolved in 65 mL ethanol in a round-bottom flask (500 mL) equipped with a reflux condenser. Distilled water (0.9 g, 0.05 mol), 1 mL hydrochloric acid, and 65 mL ethanol were mixed and then added slowly into the VTMS solution with ultrasonic stirring for

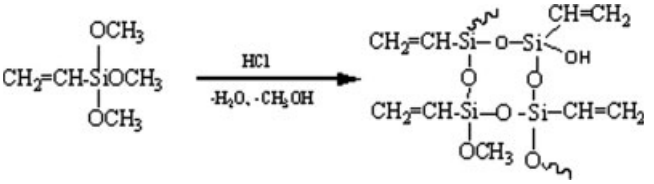

Scheme 1 Hydrolysis reactions of VTMS.

20 min. The pH of the solution was adjusted to 2 by adding hydrochloric acid (37%) dropwise. The mixture was allowed to react under magnetic agitation at ambient temperature for 6 h, then continued to react for another 42 h at 65°C. Finally, the solvent, water, and excess VTMS monomer were removed under reduced pressure at 60°C for 1 h. The hydrolysis reaction of VTMS is illustrated in Scheme 1.

The resultant products were characterized by ^{1}H NMR and FTIR. The average molecular weight by GPC was $M_n = 1907$, and the polydispersity was PDI = 1.49.

Synthesis of acrylated polyester

A typical polycondensation technique[34] was used to prepare an acrylated polyester resin. The chemical structure of 1,4-CHDM, NPG, HD, ADA, and MA are illustrated below. The formulation of the acrylated polyester is listed in Table I.

The synthesis process, reported previously, consisted of two steps. The average molecular weight was found to be $M_n = 2420$, with a PDI = 2.4 via GPC. The acid number and hydroxyl number were measured according to ASTM standards D 1639 and D 4274-94, respectively. There was a mixture of possible chemical structures for the acrylated polyester. The following are the possible chemical structures of acrylated polyester.

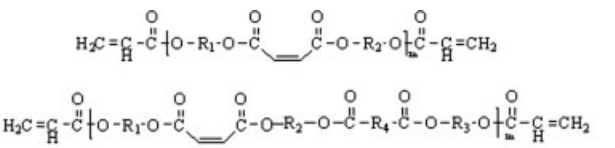

((1, 4-CHDM : HO-R$_1$-OH), (NPG : HO-R$_2$-OH), (1, 6-HD : HO-R$_3$-OH) and (ADA : HOOC-R$_4$-COOH))

Hybrid coatings formulation and preparation

The UV-curable hybrid coatings were formulated using an acrylated polyester resin (PA), VTMS oligomer, and photoinitiator (Ciba Darocur 4265). The formulations are shown in Table II.

TABLE I
Formulation of Acrylated Polyester

Diol (mol)	Diacid (mol)	Acrylic acid (mol)
1,4-CHDM: 1.5 NPG: 2 1,6-HD: 2	MA: 2.3 ADA: 1.2	AA: 4

TABLE II
The Formulation of Acrylated Polyester with Differing Contents of VTMS oligomer

AP/VTMS films	Acrylated polyester (wt %)	VTMS oligomer (wt %)	Photoinitiator (wt %)
0	96	0	4
1	91	5	4
2	86	10	4
3	81	15	4
4	76	20	4
5	66	30	4

Each mixture was mixed on a roller mill for 24 h, then cast on aluminum panels (alloy 3003 H14, Q-Panel Lab Products) by a drawdown bar with a thickness of 3 mils. Aluminum panels were degreased with acetone before casting the films. The films were cured by a Fusion UV-System Processor (P300) with a belt speed of 10 ft/min (Mercury arc bulb, 150 mW/cm^2).

The photoinitiator used consists of 50% 2,4,6-trimethylbenzoyl-diphenyl-phosphine oxide and 50% 2-hydroxy-2-methyl-1-phenyl-propan-1-one. Their structures are shown below.

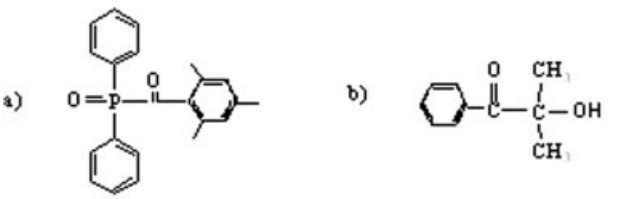

a) 2, 4, 6-trimethylbenzoyl-diphenyl-phosphine oxide
b) 2- hydroxy-2-methyl-1-phenyl-propan-1-one

Instruments and testing methods

Thermal property of hybrid films was measured on a thermogravimetric analysis (TGA) Q500 (TA Instruments) with a heating rate of 10°C/min in air. The average weight of the samples was 6–10 mg. Contact angles were measured using a Ram Hart NRL-100 contact angle gonimeter equipped with an environmental chamber. Advancing and receding angles were determined using the static method and were performed on films, which were cast on aluminum panels.

The viscoleatic properties were determined on a dynamic mechanical thermal analyzer (DMTA V, Rheometrics Scientic) with a frequency of 1 Hz and a heating rate of 4°C/min over a range of −50 to 200°C. The film geometry was 5 × 25 mm^2 with a thickness

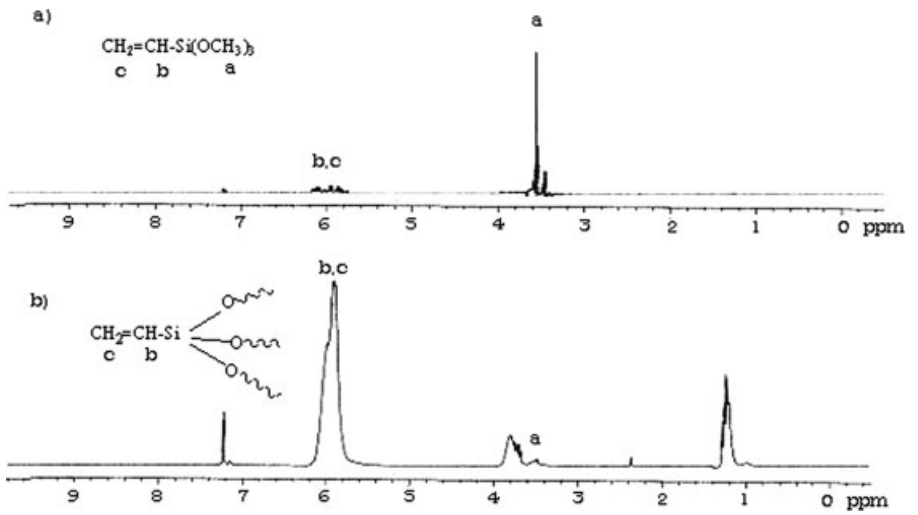

Figure 1 ^{1}H NMR spectra of VTMS (a) VTMS monomer and (b) VTMS oligomer (reaction 48 h).

of 102–112 μm. Fracture toughness was performed using the instrument designed by the Soucek laboratory. The dimensions of films were 0.05–0.065 mm in thickness and 14–16 mm in width. Each film was cut with a razor blade to create the edge notch. Six samples were tested for each film. The plane-stress fracture toughness (K_c, stress intensity factor at fracture) was calculated using the following equation:[35]

$$K_c = \sqrt{3.94\left(\frac{2w}{\pi a}\right)\tan\left(\frac{\pi a}{2w}\right)}\sqrt{a}\left(\frac{F}{[w-a]b}\right)$$

where w is the specimen width, b is specimen thickness, a is notch depth, and F is the load at which creak propagation begins. The energy release rate per unit creak area at fracture (G_c) can be calculated by the following equation:[35,36]

$$G_c = {K_c}^2/E$$

where E is the tensile modulus. Each reported value for the fracture toughness represents the average value of five samples.

The tensile properties were measured using an Instron 5567 (Instron) according to the ASTM D 2794-84 standard. The dimensions of the films used for tensile testing were 0.05–0.065 mm thick and 14–16 mm wide. Six samples were tested for each film. The crosshead speed was 5 mm/min. Surface rubbing abrasion resistance of films was measured by the Taber Abraser Test using a Taber Model 5130 Digital Abraser with LED Readouts from Elcomter Company. Test cycle was 200. Impact resistance was performed on a TQC Impact Rester (ASTM 2794-84). Pull off adhesion was tested using an Elcometer 106 Adhesion Tester (ASTM D 4541-85). Pencil hardness was tested according to ASTMD 3363-74 standard.

^{1}H NMR spectra were recorded on a Gemini-300 spectrometer (Varian). Fourier Transform infrared spectroscopy (FTIR) was recorded on an ATI Mattson Genesis FTIR spectrometer. Matrix-assisted laser desorption/ionization time-of-flight (MALDI-TOF) mass spectrometry experiments were performed using a Bruker (Billerica, MA) Reflex III MALDI-TOF mass spectrometer. Molecular weight and its distribution were determined by gel permeation chromatography (GPC).

Atomic force microscopy (AFM) was performed to observe the morphology of the hybrid film using a multimode scanning microscope (Digital Instrument Nanoscope III a) in a tapping mode with a silicon tip. Test samples were prepared by mixing VTMS colloid and acrylated polyester on a roller mill for 24 h, then casting the samples on glass panels by a drawdown bar.

RESULTS AND DISCUSSION

The overall objective of this study was to investigate the effects of incorporating a VTMS oligomer in UV-curable organic/inorganic hybrid coatings. It was anticipated that a high UV-curing activity and hyperbranched crosslinking and penetration of VTMS/AP would lead to improved film performance compared to a slower curing and lower crosslink density system. Five levels of VTMS (0, 5, 10, 15, and 20 wt %) were used in this study to evaluate the effects of the VTMS oligomer on the final film properties. The VTMS structure contains siloxane- and vinylfunctional-group; therefore, VTMS colloids provide the control of cluster size and UV-crosslinkable functional group, which can couple the inorganic to the organic phase. In addition, it was thought that the size of the colloid could be better controlled, than TEOS derived colloids by virtue of the silane functionality.

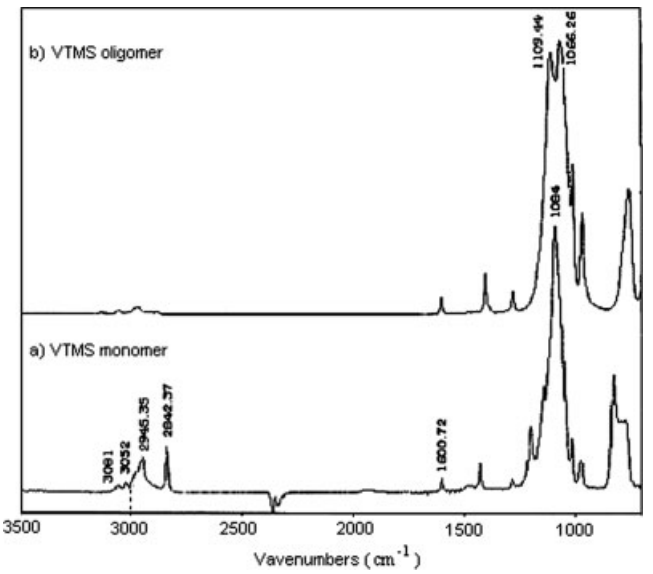

Figure 2 Comparison of FTIR spectra of (a) VTMS monomer and (b) VTMS oligomer.

Figure 1 represents the ^{1}H NMR spectra of the VTMS monomer [Fig. 1(a)] and its hydrolysis and condensation products [Fig. 1(b)]. In the ^{1}H NMR spectrum of the VTMS monomer, the resonances of the methoxy groups at δ 3.55 ppm were very strong. The hydrolysis and condensation of the VTMS was indicated by a sharp diminish of the resonance of the methoxy group at δ 3.55 ppm coupled with an increase of the broad of resonance at δ 5.9–6.1 ppm (H_c and H_b in the CH_2=CH-group) [Fig. 1(b)]. After reacting for 48 h, almost all of the methoxy groups had reacted as indicated by the greatly diminished signal for the methoxy resonance. Dubitsky et al. used ^{1}H NMR spectroscopy to investigate the hydrolysis of VTMS.[37] During hydrolysis, the replacement of alkoxy groups on the silicon atoms did not occur on all the alkoxy units at once but seemed to proceed gradually, faster for the monosubstitution than for the di- and trisubstititution. In fact, in 4 h, the monohydrolyzed product formed,[37] and a signal appeared at ~5.05 ppm in 48 h, two additional signals should be observed from 4.53 to 4.77 ppm, due to di- and then trihydrolyzed species. However, three resonances disappeared by presaturating the water signal [shown in Fig. 1(b)]. Silanol signals were not detected in acidic condition for two main reasons: acid catalyze fast exchange between protons and water, and quickly occurred condensation prevents the accumulation of SiOH groups.

Figure 2 shows the comparison of FTIR spectra of the VTMS monomer and the VTMS oligomer after reaction for 48 h. In the FTIR spectrum of the VTMS monomer [Fig. 2(a)], the absorbance at 2945 and 2842 cm^{-1} were attributed to —CH_3 stretching bands. The band at 3052 cm^{-1} was due to the C—H stretching of the C=C—H group, and the bands at 1600 and 3081 cm^{-1} were due to the CH=CH stretching. The strong band at 1084 cm^{-1} is indicative of Si—O—CH_3 stretching. In the spectrum collected after the reaction [shown in Fig. 2(b)], the intensity of the 2945 and 2842 cm^{-1} bands decreased sharply indicating the consumption of the methoxy groups in the reaction. New bands at 1109 and 1066 cm^{-1} appeared which was indicated of the Si—O—Si network. The study of structure of the VTMS oligomers indicated that the VTMS oligomer existed in four structures: linear, branched (containing some or no linear sections), cyclized (or cycle-containing) (containing some or no linear sections), and a combined cyclized-branched structure. Linear structures have close to the same mass as their corresponding branched structures.[11]

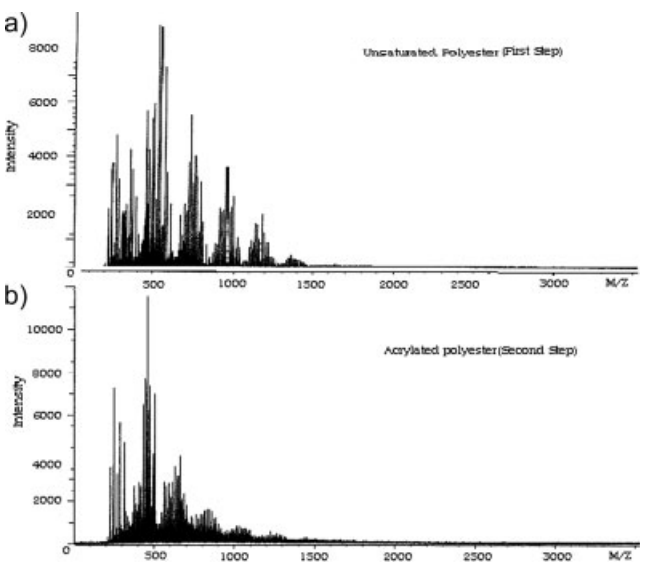

Figure 3 MALDI-TOF mass spectra of (a) unsaturated polyester and (b) acrylated polyester.

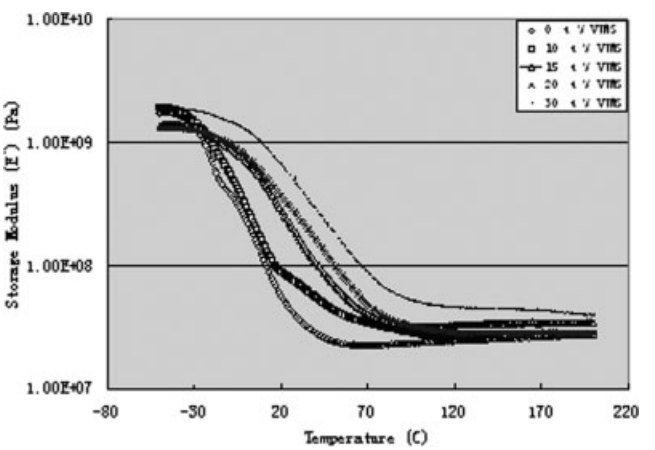

Figure 4 Storage modulus (E') of the hybrid films as a function of VTMS oligomer content.

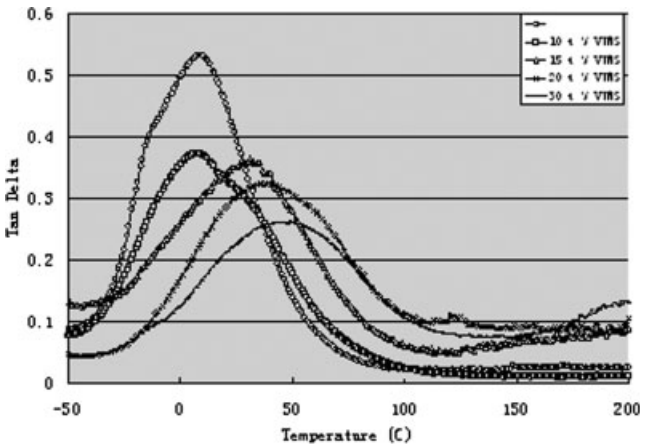

Figure 5 Tan delta (δ) of the hybrid films as a function of VTMS oligomer content.

Figure 3 shows the MALDI-TOF mass spectra of the unsaturated polyester and the acrylated unsaturated polyester. For the unsaturated polyester, peaks below 2500 Da were observed, possibly due to a high polydispersity (PD > 1.2) of the sample.[38] Peaks in the lower molecular weight range (e.g., observed *m/z* 325.17, 461.07, 537.24, and 707.32) were unequivocally attributed to oligomers containing MA. In the higher observed molecular weight region, *m/z* values of many other observed peaks corresponded to the theoretical calculated masses of oligomers containing MA (e.g., observed *m/z* 931.38, 1181.49, 1339.58, 1563.74, 1629.77, respectively); There was enough evidence in the mass spectral data to state with confidence that there was incorporation of the maleic anhydride monomer in the polyester across the entire mass range.

For the acrylated unsaturated polyester, only the lower masses below 3500 Da were observed because of the high polydispersity of the sample (PD = 2.2 by GPC).[38] Peaks in the lower molecular weight range (below *m/z* 900) showed incorporation of either one or two terminal acrylic acid groups. Peaks observed in the higher molecular weight range of the acrylated polyester also showed terminal acrylic acid groups. This provided evidence that acrylic polyester contains the MA- and the AA-terminated structures.

Dynamic mechanical property

Dynamic mechanical thermal analysis (DMTA) of thin films provides the information of crosslink density, glass transition temperature (T_g), and extent of cure. The crosslink density (ν_e) is the number of moles of elastically effective network chains per cubic centimeter of material. The viscoelastic properties of the hybrid films as a function of VTMS oligomer content are shown in Figures 4 and 5. There is a rubbery plateau at >70°C for all of the samples indicating a crosslinked network. Higher concentrations of VTMS oligomers tended to shift the transition to a higher temperature. Also the increasing VTMS oligomer content broadened the transition region, and ultimately, increased the storage modulus. At 20°C the storage modulus (E') of the organic film was 1.7×10^7 Pa, while the E' of the hybrid film with 20 wt % VTMS oligomer loading was 1.95×10^8 Pa, more than 10 times higher than that of the organic film.

The crosslink density of the films was calculated with the following equation:[39,40]

$$E' = 3\,\nu_e RT$$

where ν_e is the number of moles of elastically effective chains per cubic centimeter of the film, E' is the storage modulus in the rubbery plateau, R is the gas constant, and T is the temperature in K corresponding to the storage modulus value. It is important to note that this relationship was not the developed for organic/inorganic hybrid systems. However, a better model to predict crosslink density for these systems is currently unavailable. Consequently, this model is used with the caveat that organic crosslinks and organic/inorganic crosslinks are part of the calculation are not differentiated. Table III shows the crosslink density and glass transition temperature (T_g) of the hybrid films as a function of VTMS oligomer content. The glass transition temperature (T_g) was determined from the maximum tan δ and increased from 9.1°C to 70.2°C as the VTMS oligomer content increased from 0 to 30 wt %. An increase in crosslink density was observed when VTMS oligomer was introduced. When compared with the organic film,

TABLE III
Viscoelastic Properties of the Hybrid Films as a Function of VTMS Oligomer

Hybrid films	VTMS oligomer (wt %)	Film thickness (μm)	Glass transition temparature, T_g (°C)	Crosslink density (mol/m^3) (×10^3)	E' (Pa) (10^7) (beyond T_g 80 °C)
0	0	102.6	9.1	2.58	2.33
1	10	105.5	8.1	3.38	3.04
2	15	112.2	31.2	3.46	3.24
3	20	106.3	37.2	3.47	3.23
4	30	106.6	70.2	4.25	4.46

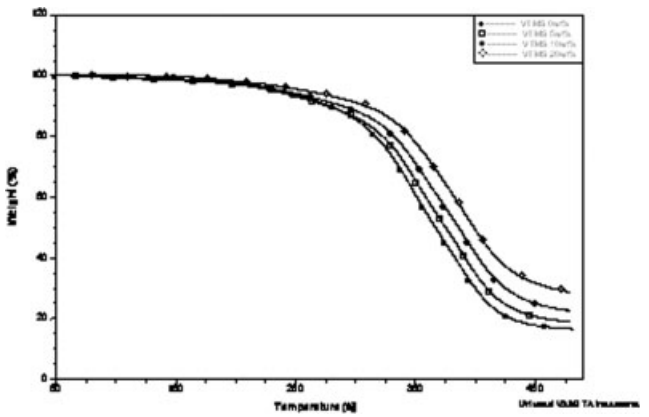

Figure 6 Thermal gravimetric curves of VTMS/acrylated polyester hybrid films.

the crosslink density with 10 wt % VTMS oligomer loading increased by 31%. The highest crosslink density (4.25 mol/cm^3) was found at 30 wt % of VTMS oligomer loading, which was 64.7% higher than that of the organic film.

Crosslink density has a direct impact on the tan δ. Figure 5 shows that the height of the tan δ peak decreased, the apex of the peak (corresponding to T_g) shifted to a higher temperature, and the peak was broadened as the loading content of VTMS oligomer increased. This is because the increasing of crosslink density reduces long range segment motion required for viscous flow behavior. Therefore, the cure extent of the hybrid films increased. The area under the tan δ curve can also be used to measure the extent of cure.[39,40] It was calculated from Figure 5 that the area under the tan δ curve decreased as the loading content of VTMS oligomer increased, which further indicated the increasing of the degree of cure.

The increased storage modulus, crosslink density, T_g, and degree of cure were all attributed to the intramolecular reactions of the VTMS oligomer and the intermolecular reaction between the VTMS colloid and acylated polyester. The acrylated VTMS oligomer functioned as a hypercrosslinker which coupled the inorganic segment to the organic phase. As a result, a crosslink network between the inorganic and organic phases enhanced the overall performance of ceramer films and altered the mechanical properties.

Thermal properties

Thermal gravimetric analysis (TGA) was used to evaluate the thermal stability of the hybrid coatings as a function of VTMS oligomer content. Figure 6 shows the effect of varying VTMS oligomer loading on the thermal degradation of VTMS/acrylated polyester hybrid films. At low temperature (<170°C), the VTMS oligomer concentration had no major impact on the hybrid films thermal stability. Variations in stability were not observed until higher temperatures (>170°C). There was a shift to slightly higher temperatures as the VTMS oligomer loading increased. The hybrid films showed delayed decomposition when compared with the organic film. A 10% weight loss was observed in the organic acrylated polyester film at 258°C, whereas the 20 wt %VTMS hybrid film did not show 10% weight loss until 268°C. The rapid weight loss for organic film began at 260°C, while this did not occur in the 20 wt % VTMS hybrid film until 270°C. Hybrid films showed higher thermal stability than the organic film, which may have resulted from the high thermal stability of silica and the crosslink point nature of the silica colloids.

Surface properties

Surface properties of films, such as smoothness, surface tension, and adhesion are very important factors affecting coating industrial applications and have a close relationship with the contact angle of coatings. Figure 7 shows the contact angle and surface tension of hybrid films as the function of VTMS oligomer content. On substrates, contact angle measurements were performed with doubly distilled water on

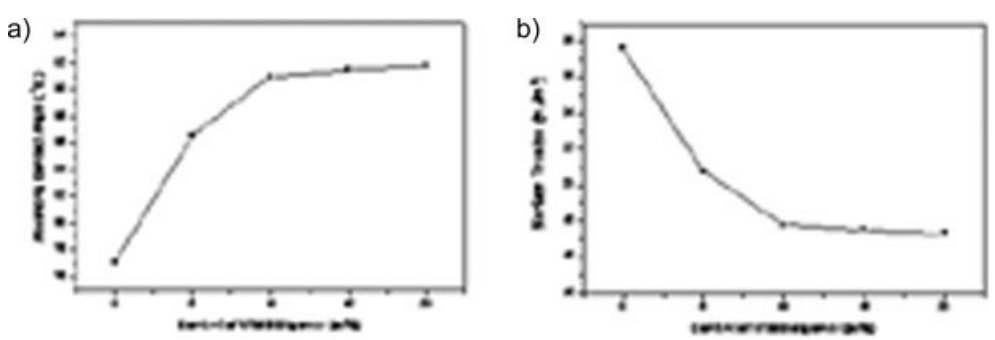

Figure 7 Contact angle and surface tension of UV-cured VTMS/AP hybrid films; (a) contact angle and (b) surface tension.

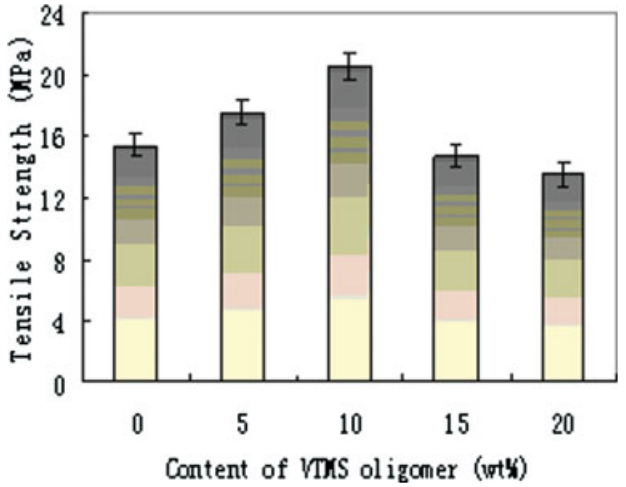

Figure 8 Tensile strength of the hybrid films. [Color figure can be viewed in the online issue, which is available at www.interscience.wiley.com.]

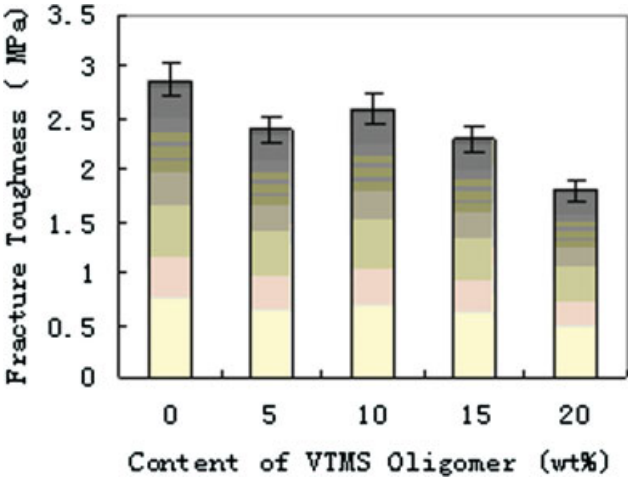

Figure 10 Fracture toughness (K_c) of the hybrid films. [Color figure can be viewed in the online issue, which is available at www.interscience.wiley.com.]

VTMS/acrylated polyester films. For the organic acrylated polyester film, the contact angle was 77°. After the VTMS oligomer was added, the wettability increased sharply and reached 91° at 10 wt % VTMS oligomer loading. At low content of VTMS oligomer, as VTMS content increased the contact angle of the films increased very quickly as shown in Figure 7(a).

Surface tension of the hybrid films can be calculated from contact angles using the following equation:[41]

$$\text{Cos}\ \theta = -1 + 2\sqrt{\frac{\gamma}{\gamma_{lv}}}\, e^{-\beta(\gamma_{lv}-r)}$$

where θ is the contact angle, γ_{lv} is the surface tension of liquid-vapor (water: 72.7 mJ/m^2), and β is 0.0001247 (m^2/mJ)^2. Results show that the incorporation of VTMS into acrylated polyester increased the contact angle of the films and led to a clear decrease in the surface tension. Also, as it was anticipated, films surface appearance improved evidently.

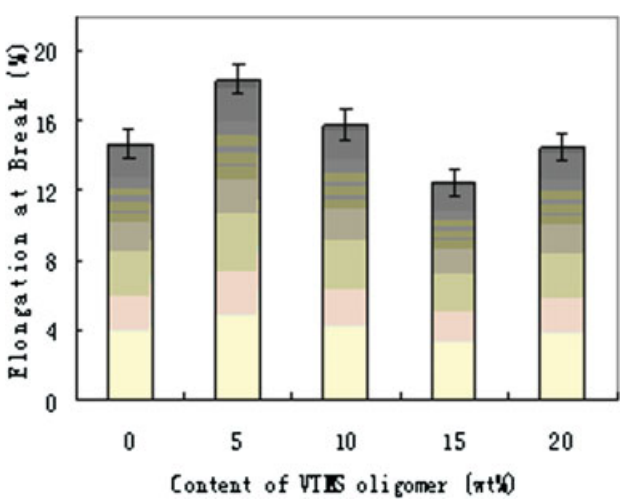

Figure 9 Elongation at break of the hybrid films. [Color figure can be viewed in the online issue, which is available at www.interscience.wiley.com.]

Tensile properties and fracture toughness

Figures 8 and 9 showed the tensile strength and elongation at break as a function of VTMS colloids content. The tensile strength (shown in Fig. 8) shows an initial increase in tensile strength from 0 to 5 wt % VTMS colloids, and a large increase from 15.4 MPa to maximum of 20.5 MPa at 10 wt % VTMS colloids content. This is attributed to the intimate interaction between the reinforcing inorganic colloids in the organic matrix. The tensile strength decreased to 14.3 MPa when VTMS colloids content increased to 20 wt %. This could be due to the aggregation of VTMS colloids which caused stress induced cracks, resulting in a reduction in tensile strength. It is very interesting to note that the lowest elongation at break was obtained for the hybrid which contained 15 wt % VTMS colloids content (shown in Fig. 9). This is nanometer-effect of inorganic particles and their dispersions at low concentration of VTMS colloids. Therefore, at low VTMS colloids loading with uniform particle dispersions on both and tensile strength and elongation of the hybrid film were improved.

The fracture toughness (K_c) and energy release rate (G_c) of the hybrid films are shown in Figures 10 and 11, respectively. Fracture toughness and energy release rate are the measurements of resistance to crack extension. The fracture toughness of the hybrid films shows a little decrease when VTMS colloids content increased from 5 to 20 wt %. Energy release rate (G_c) of the hybrid films shows the same trend except for 15 wt % VTMS colloids content. There is a

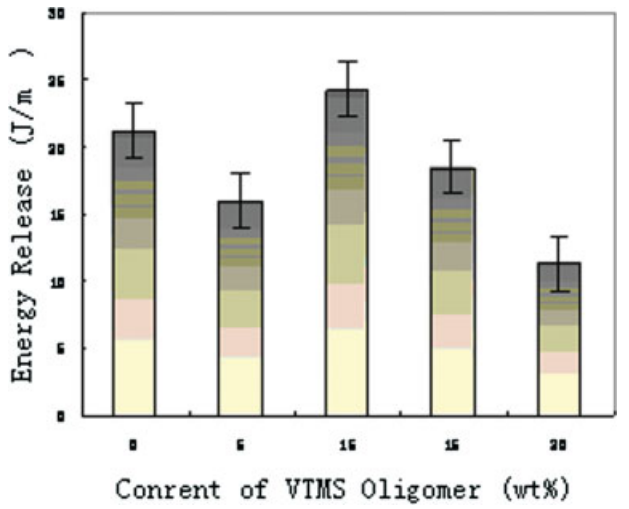

Figure 11 Energy release rate per unit creak area at the fracture (G_c) of hybrid films. [Color figure can be viewed in the online issue, which is available at www.interscience.wiley.com.]

large increase of energy release rate for the hybrid films at 15 wt % VTMS colloids content. The data of fracture toughness and energy release rate indicated that the VTMS colloids enhanced the resistance to crack extension of the hybrid films and then can give optimum content of VTMS colloids for the hybrid films existed.

Coating properties

One of the likely industrial applications of hybrid coatings is topcoats. The enhancement of surface abrasion resistance, hardness, adhesion, and impact resistance are important for its application.

Table IV shows the general mechanical properties of the hybrid film as a function of VTMS colloids concentration. The pencil hardness increased when the VTMS colloids content was increased. However, the abrasion weight loss decreased. Because of the high hardness of VTMS colloids, the strong interaction and interpenetrated nature between chain of organic phase and inorganic particles make the high pencil hardness of hybrid film. The alkene functionalized VTMS oligomer of the organic phase increased crosslink density, and the inorganic silica particles also possess an inherent hardness and abrasion resistance. Further, the improvement of scratch and abrasion resistance of such hybrid coatings was impressive with higher content of VTMS oligomer. However, the high content of inorganic phase is limited by the impact resistance of the films.

As the content of the VTMS oligomer increased, the pull off adhesion increased and reached a maximum at 15 wt % VTMS loading. The enhancement of adhesion has been attributed to both the chemical bonding between the Si—OH groups and the Al—OH on the aluminum substrate with the forming of a Si—O—Al linkage and hydrogen bonded on the substrate.[29] With the presence of VTMS oligomer, the film surface quality was also improved. The effect of modification depended on the appropriate content of the VTMS oligomer.

The falling impact indenters are normally the most severe due to the ''shock'' nature of the test. The bending and stretching of the aluminum panel base on which a coating was applied provided valuable information on the plastic and adhesion characteristics of the coating. As the content of VTMS oligomer increased, the impact resistance only decreased marginally. That may be attributed to the increase in crosslink density of the organic phase which reduced the flexibility of the hybrid system. Since the inorganic phase is the discontinuous phase, it does effect the bulk properties of the coating until ~20 wt %.

The comparison of TEOS oligomer based hybrid systems and VTMS colloid based hybrid system indicated that the photo polymerization activity of TEOS/acrylated polyester system was tested by Photo-DSC at similar formulation to VTMS/acrylated polyester system.[9] For VTMS hybrid formulations, the time to reach the exotherm peak was 0.04 min, three times faster than the time for TEOS hybrid formulations (0.15 min). The integrated exotherm of VTMS/acrylated polyester was over two times greater than that of corresponding TEOS/acrylated polyester film. And the slope to reach the exotherm peak for VTMS system is very steep, while for TEOS/acrylated polyester system, it is gradual. It means that the polymerization of VTMS/acrylated polyester system is much higher than that of TEOS/acrylated

TABLE IV
Coating Properties of Hybrid Films with Various Concentrations of VTMS

	Pencil hardness	Taber abrasion weight loss (mg)	Pull off adhesion (MPa)	Direct impact resistance (kg/cm^2)	Inverse impact resistance (kg/cm^2)
AP/VTMS 0	1 H ± .3	5.6	0.92	67.5	62
AP/VTMS 1	2 H ± .3	4.3	1.05	63	57
AP/VTMS 2	3 H ± .5	3.2	1.1	62	55
AP/VTMS 3	4 H ± .5	3	1.28	60	51
AP/VTMS 4	5.5H ± .5	3	1.2	56	50

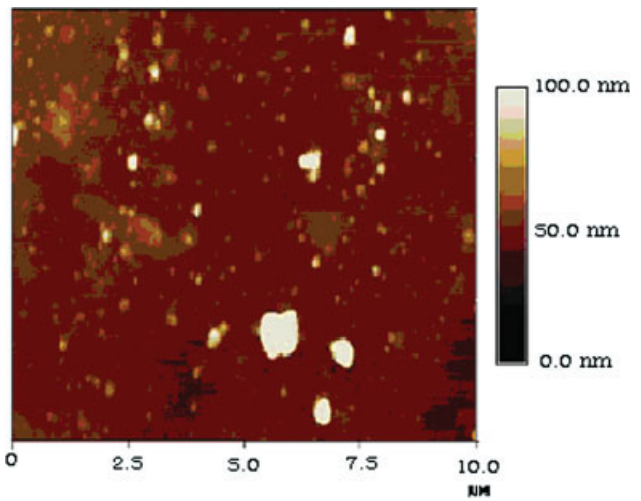

Figure 12 AFM of the hybrid film of VTMS/AP. [Color figure can be viewed in the online issue, which is available at www.interscience.wiley.com.]

polyester system, which may be attributed to the structure difference of TEOS oligomer and VTMS colloid. The are double bonds with VTMS structure, thus adding of VTMS not only reduced the viscosity of the formulation and increased the mobility of the organic polymer chain during propagation but also provided additional double bonds, which participated as a hybrid crosslinker during the free radical photo-polymerization.

Morphology of hybrid film

The morphology of VTMS/AP hybrid film was observed using atomic force microscopy (AFM) as shown in Figure 12. The bright spots with varied shapes are silica particles which were dispersed throughout the cured hybrid films. The average silica particle size is around 90 nm. Larger silica particles around 200–300 nm were also observed. AFM imaging indicated that the hybrid films of VTMS/AP had microphase separation, and VTMS silica-colloids were dispersed mostly at the nanometer level and only part of aggregation. The aggregation sizes are from nanometer to micrometers.

The formation of VTMS/AP hybrid films involved homopolymerization of the VTMS oligomer and AP, and copolymerization between both components. Based on AFM data and analysis of the polymerization mechanism of a VTMS/AP system, a schematic model for UV-curing VTMS/AP hybrid films was proposed and is shown in Scheme 2. This model displays silica clusters crosslinked organic matrix by chemical bond, and the silica clusters interconnected via the organic phase. The formation VTMS/acrylated polyester hybrid films involve a simultaneous polymerization of the reactive group in both the organic and inorganic phase. The scattered small regions represent the silicate rich domains, and the connecting lines represent the organic polymers. The polymerization is concomitant homopolymerization of VTMS colloid or acrylated polyester and copolymerization. The functional group of —Si—CH=CH_2 which distributes throughout the inorganic particles can bond the inorganic particles to the organic phase. Therefore, the rate of UV-curing polymerization and crosslink density can be increased. This means that VTMS colloids will function as a hyperbranched crosslinker. Also, the model represents that the vinyl groups are not only on the periphery of the colloid but distribute throughout the colloid. Definitely, in addition to an inorganic siloxane formation some organic crosslinking could be expected throughout the inorganic domain. It would be reasonable to assume that the highest crosslink density would be located around the periphery of the VTMS colloids. Our results from AFM and mechanical properties support this particle-like model.

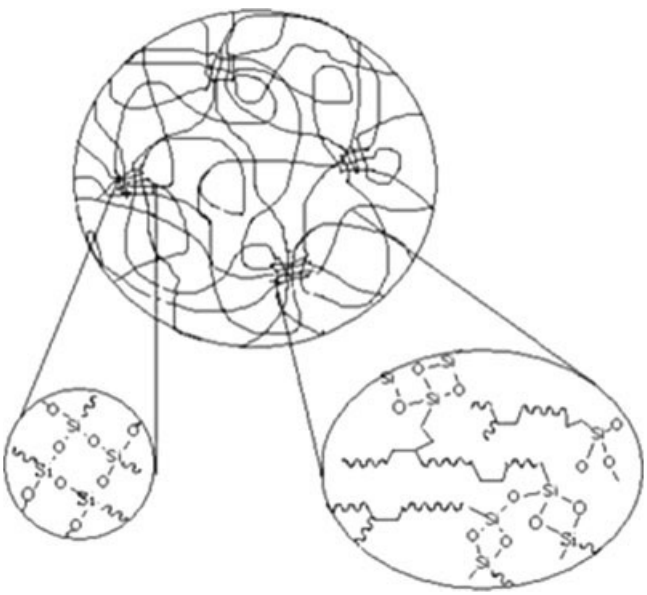

Scheme 2 A schematic model for UV-curing VTMS/AP hybrid films.

CONCLUSIONS

UV-curable organic–inorganic hybrid films based on acrylated polyester were prepared using vinylfunctionalized silica colloid. Results show that adding the VTMS oligomer could greatly improve thermal stability, as well as storage modulus, crosslink density, T_g, and extent of cure. Also the VTMS leading increased tensile strength ($\leq$10 wt %), abrasion resistance ($\leq$15 wt %), and pencil hardness. The average silica size of VTMS silica-colloids is around 90 nm and silica-colloids were dispersed mostly at the nanoscale and with

very little aggregation. It was proposed that the VTMS oligomer has the functions as a reactive diluent, crosslinker, surface modifier, and reactive inorganic filler.

References

1. Mezzenga, R.; Boogh, L.; Pettersson, B.; Manson, J. A. E. Macromolecules 2000, 33, 4373.
2. Zou, K.; Soucek, M. D. Macromol Chem Phys 2004, 205, 2032.
3. Zong, Z.; Soucek, M. D.; Xue, C. J Polym Sci Part A: Polym Chem 2005, 43, 1607.
4. Nebioglu, A.; Teng, G. H.; Soucek, M. D. J Appl Polym Sci 2006, 99, 115.
5. Zong, Z.; He, J. Y.; Soucek, M. D. Prog Org Coat 2005, 53, 83.
6. Gunji, T.; Kawaguchi, Y.; Okonogi, H.; Sakan, T.; Arimitsu, K.; Abe, Y. J Sol–Gel Sci Technol 2005, 33, 9.
7. Fouassier, J. P. Photoinitiation, Photopolymerization, and Photocurin, Fundamentals and Applications; Hanser: New York, 1995; pp 246–365.
8. Pappas, S. P., Ed. UV Curing: Science and Technology, Vol. 4; Technology Marketing Corporation: Stanford, 1978.
9. Bauer, F.; Sauerland, V.; Glasel, H. J.; Ernst, H.; Findeisen, M.; Hartmann, E.; Langguth, H.; Marquardt, B.; Mehnert, R. Macromol Mater Eng 2002, 287, 546.
10. Oksuz, M.; Yildirim, H. J Appl Polym Sci 2004, 93, 2437.
11. He, J.; Nebioglu, A.; Zong, Z.; Soucek, M. D.; Wollyung, K. M.; Wesdemiotis, C. Macromol Chem Phys 2005, 206, 732.
12. Novak, M. B. Adv Mater 1993, 5, 422.
13. Landry, C.; H. J. T.; Coltrain, B. K.; Brady, B. K. Polymer 1992, 33, 1486.
14. Wilkes, G. L.; Orler, B.; Huang, H. H. Polym Prepr 1985, 26, 300.
15. Noell, J. L. W.; Wikes, G. L.; Mohanty, D. K.; McGrath, J. E. J Appl Polym Sci 1990, 40, 1177.
16. Sabata, A.; Van Ooij, W. J.; Koch, R. J. J Adhes Sci Technol 1993, 7, 1153.
17. Gilberts, J.; Tinnemans, A. H. A. J Sol–Gel Sci Technol 1998, 11, 53.
18. Witucki, G. L. J Coat Technol 1993, 65, 57.
19. Sabata, A.; Van Ooij, W. J.; Koch, R. J. J Adhes Sci Technol 1993, 7, 1153.
20. Witucki, G. L. J Coat Technol 1993, 65, 5.
21. Klemperer, W. G.; Ramamurthi, S. D.; Brinker, C. J.; Clark, D. E.; Ulrich, D. R., Eds. Better Ceramics Through Chemistry III; Materials Research Society: Pittsburgh, PA, 1988; pp 1–13.
22. Klemperer, W. G.; Mainz, V. V.; Ramamurthi, S. D.; Rosenberg, F. S.; Brinker, C. J.; Clark, D. E.; Ulrich, D. R., Eds. Better Ceramics Through Chemistry III, Materials Research Society, Pittsburgh, PA, 1988; pp 15–24.
23. Pope, E. J. A.; Mackenzie, J. D. J Non-Cryst Solids 1986, 87, 185.
24. Sailer, R. A.; Soucek, M. D. Prog Org Coat 1998, 33, 36.
25. Ballard, R. L.; Tuman, S. J.; Fouquette, D. J.; Stegmiller, W.; Soucek, M. D. Chem Mater 1999, 11, 726.
26. Ni, H.; Simonsick, W. J., Jr.; Skaja, A. D.; Sailer, R. A.; Williams, J. P.; Soucek, M. D. Prog Org Coat 2000, 38, 110.
27. Ni, H.; Skaja, A. D.; Soucek, M. D. Prog Org Coat 2000, 38, 184.
28. Chen, J.; Soucek, M. D. Eur Polym J 2003, 505, 520.
29. Ni, H.; Skaja, A. D.; Sailer, R. A.; Soucek, M. D. Macromol Chem Phys 2000, 201, 722.
30. Zong, Z.; Soucek, M. D.; Liu, Y.; Hu, J. J Polym Sci Part A: Polym Chem 2003, 41, 3440.
31. Ni, H.; Aserud, D. J.; Simonsick, W. J., Jr.; Soucek, M. D. Polymer 1999, 40, 5675.
32. Hu, L. J.; Zhang, X. W.; Sun, Y.; Williams, R. J. J. J Sol–Gel Sci Technol 2005, 34, 41.
33. Hoyle, C. E.; Kinstle, J. F. In Radiation Curing of Polymeric Materials; Hoyle, C. E., Kinstle, J. F., Eds., ACS Symposium Series: Washington, DC, 1989; Chapter 1.
34. Derks, F.; Johannes, M. Int. Pat. Appl. WO02/055473 A1 (2002).
35. Williams, J. G. Fracture Mechanics of Polymers; Wiley: New York, 1987.
36. Hertzberg, R. W. Deformation and Fracture Mechanics of Engineering Materials, 3rd ed.; Wiley: New York, 1989.
37. Dubitsky, Y.; Zaopo, A.; Zannoni, G.; Zetta, L. Mater Chem Phys 2000, 64, 45.
38. Byrd, H. C. M.; McEwen, C. N. Anal Chem 2000, 72, 4568.
39. Hill, L. W. Prog Org Coat 1997, 31, 235.
40. Hill, L. W. J Coat Technol 1992, 64, 27.
41. Kwok, D. Y.; Neumann, A. W. Adv Colloid Interf Sci 1999, 81, 167.